

# Optimizing Organic Functionality in Mesostructured Silica: Direct Assembly of Mercaptopropyl Groups in Wormhole Framework Structures

Yutaka Mori and Thomas J. Pinnavaia\*

Department of Chemistry, Michigan State University, East Lansing, Michigan 48824

Received January 19, 2001. Revised Manuscript Received March 25, 2001

A series of mercaptopropyl-functionalized wormhole mesostructures, denoted MP-HMS, have been prepared through the  $S^{0T0}$  assembly of alkylamine surfactants ( $S^0$ ) and mixtures of 3-mercaptopropyltrimethoxysilane and tetraethyl orthosilicate as framework precursors ( $I^0$ ). Unprecedented levels of organo functionalization, corresponding to at least 50% of the silicon sites, were achieved while retaining well-expressed mesostructures with pore sizes, pore volumes, and surface areas as high as 2.8 nm, 0.69 cm<sup>3</sup>/g, and 1225 m<sup>2</sup>/g, respectively. Also, up to ~90% of the framework silicon sites could be fully cross-linked, lending exceptional hydrothermal stability to the mesostructures. The key to highly functionalized MP-HMS derivatives lies in the use of long-chain alkylamine surfactants as structure directors (e.g., octadecylamine) in combination with a relatively high assembly temperature (e.g., 65 °C) and a high-polarity water–ethanol solvent. Increasing the assembly temperature increased both the framework pore size and the degree of framework cross-linking, whereas increasing the MP content lowered the pore size while improving the framework cross-linking. The effects of assembly temperature and MP loading were attributable to changes in hydration at the H-bonded  $S^{0T0}$  interface and concomitant changes in the surfactant packing parameter. Highly functionalized MP-HMS derivatives are promising materials for use as heavy-metal ion-trapping agents and as precursors for sulfonic-acid-functionalized mesostructured catalysts.

## Introduction

Mercapto-functional mesoporous molecular sieve silicas have received considerable attention as heavy-metal ion-trapping agents.<sup>1–10</sup> The anchored thiol groups also can be oxidized to provide sulfonic acid functionality for applications in solid acid catalysis.<sup>9,11–15</sup> The potential use of these derivatives as well as other organo-

functional derivatives depends critically on the loading of accessible functional groups into the framework. To date, open framework mesostructures have been obtained for compositions in which fewer than 30% of the silicon centers have been functionalized. Therefore, there is a need to devise methods for increasing the loading of mercapto and other functional groups while maintaining the mesoporous framework structure.

Several mercaptopropylsilyl-functionalized mesostructures have been prepared through direct assembly pathways<sup>9,16,17,15</sup> as well as through grafting reactions of pre-assembled frameworks<sup>1,3–5,10</sup> using 3-mercaptopropyltrimethoxysilane (MPTS) as the functionalizing agent. In general, direct assembly pathways are preferred over grafting methods, in part, because direct assembly pathways afford a more uniform distribution of organo groups on the framework walls. Also, direct assembly allows for better cross-linking of the silane moiety to the silica framework. For instance, 20–30% of the framework silicon centers in hexagonal SBA-15<sup>15</sup> and MCM-41<sup>9</sup> mesostructures have been functionalized with mercaptopropyl groups through the direct assembly of MPTS and tetraethyl orthosilicate (TEOS) mixtures. Also, mercaptopropyl-functionalized HMS silicas with wormhole framework structures, denoted

(1) Feng, X.; Fryxell, G. E.; Wang, L.-Q.; Kim, A. Y.; Liu, J.; Kemner, K. M. *Science* **1997**, *276*, 923.

(2) Chen, X.; Feng, X.; Liu, J.; Fryxell, G. E.; Gong, M. *Sep. Sci. Technol.* **1999**, *34*, 1121.

(3) Mattigod, S. V.; Feng, X.; Fryxell, G. E.; Liu, J.; Gong, M. *Sep. Sci. Technol.* **1999**, *34*, 2329.

(4) Mercier, L.; Pinnavaia, T. J. *Adv. Mater.* **1997**, *9*, 500.

(5) Mercier, L.; Pinnavaia, T. J. *Environ. Sci. Technol.* **1998**, *32*, 2749.

(6) Mercier, L.; Pinnavaia, T. J. *Microporous Mesoporous Mater.* **1998**, *20*, 101.

(7) Brown, J.; Mercier, L.; Pinnavaia, T. J. *Chem. Commun.* **1999**, 69.

(8) Brown, J.; Richer, R.; Mercier, L. *Microporous Mesoporous Mater.* **2000**, *37*, 41.

(9) Lim, M. H.; Blanford, C. F.; Stein, A. *Chem. Mater.* **1998**, *10*, 467.

(10) Liu, A. M.; Hidajat, K.; Kawi, S.; Zhao, D. Y. *Chem. Commun.* **2000**, 1145.

(11) Van Rhijin, W. M.; De Vos, D. E.; Sels, B. F.; Bossaert, W. D.; Jacob, P. A. *Chem. Commun.* **1998**, 317.

(12) Bossaert, W. D.; De Vos, D. E.; Van Rhijin, W. M.; Bullen, J.; Grobet, P. J.; Jacob, P. A. *J. Catal.* **1999**, *182*, 156.

(13) Harmer, M. A.; Sun, Q.; Michalczyk, M. J.; Yang, Z. *Chem. Commun.* **1997**, 1803.

(14) Harmer, M. A.; Farneth, W. E.; Sun, Q. *Adv. Mater.* **1998**, *15*, 1255.

(15) Margolese, D.; Melero, J. A.; Christiansen, S. C.; Chmelka, B. F.; Stucky, G. D. *Chem. Mater.* **2000**, *12*, 2448.

(16) Fowler, C. E.; Burkett, S. L.; Mann, S. *Chem. Commun.* **1997**, 1769.

(17) Hall, S. R.; Fowler, C. E.; Lebeau, B.; Mann, S. *Chem. Commun.* **1999**, 201.

MP-HMS, have been prepared through analogous assembly methods.<sup>7,18,19</sup>

When assembled from highly polar solvents, HMS mesostructures typically form spongelike particles through the intergrowth of mesoscopic wormhole framework domains. Consequently, the framework sites of HMS silicas are generally more accessible for metal ion trapping and chemical catalysis in comparison to their hexagonal SBA-15 and MCM-41 counterparts with the same framework pore size, but with highly monolithic particle morphologies. On the basis of earlier literature reports,<sup>7,18,19</sup> however, the assembly of MP-HMS mesostructures appears to limit the degree to which MP groups functionalize the framework. Little or no mesostructure formation was realized, for instance, at MP loadings above about 25 mol %.<sup>18</sup>

In the present work we have elucidated the factors that mediate the framework pore sizes and pore volumes of MP-HMS silicas prepared through a direct assembly pathway. Our results show that highly accessible mesoporous wormhole framework structures can be assembled at MP loadings of at least 50%, and even up to ~60 mol % in some cases, through favorable choices of the structure-directing surfactant and assembly conditions. These results hold important implications for use of these MP-HMS derivatives as metal ion trapping agents and as supported sulfonic acid reagents.

### Experimental Section

**Materials.** Tetraethyl orthosilicate (TEOS), 3-mercaptopropyltrimethoxysilane (MPTS), and all alkylamine surfactants were purchased from Aldrich Chemical Co. These reagents were used as-received without further purification. Deionized water and absolute ethanol were used in the synthesis and surfactant extraction processes, respectively.

**Synthesis.** The synthesis of mercapto-functionalized HMS silicas was carried out by first dissolving 2.2 mmol of the desired alkylamine surfactant in 2.3 g of ethanol at 65 °C and then diluting the surfactant solution with 29 mL of water preheated at 65 °C. The surfactant solution was then shaken in a reciprocating water bath at the desired assembly temperature for a period of 30 min. A 10-mmol quantity of a  $x$ MPTS and  $(1 - x)$ TEOS mixture where  $x$  equals the molar fraction of total silicon present as mercaptopropyl silane was then added to the surfactant solution. The reaction vessel was sealed, and the mixture was allowed to age with stirring for 72 h. The resulting product was filtered and air-dried for 24 h. Surfactant removal from the as-made mesostructure was accomplished by Soxhlet extraction for a period of 24 h using ethanol as the solvent. The ethanol-extracted product was then allowed to dry in air before use.

**Characterization.** The physical properties of the MP-functionalized silicas were determined using X-ray diffraction (XRD), nitrogen adsorption-desorption, <sup>29</sup>Si MAS NMR spectroscopy, and transmission electron microscopy (TEM). Powder XRD patterns were recorded on Rigaku rotaflex diffractometer using Cu K $\alpha$  radiation. Nitrogen adsorption-desorption isotherms were measured at -196 °C on a Micrometrics ASAP 2010 sorptometer, the samples being outgassed for 12 h at 120 °C and 10<sup>-6</sup> Torr prior to measurement. The <sup>29</sup>Si MAS NMR spectra were recorded on a Varian VRX 400-MHz spectrometer at 79.5 MHz using 7-mm zirconia rotors and a magic-angle spinning speed of at least 4.0 kHz. A pulse delay of 400 s was used to ensure full relaxation of the nuclei prior to each scan. TEM images were obtained on a JEOL 100CX microscope with

a CeB<sub>6</sub> filament and an accelerating voltage of 120 kV. Samples were prepared by sonicating the powdered samples for 20 min in ethanol and then evaporating two drops onto carbon-coated copper grids.

### Results

**MP-HMS Mesostructure Assembly.** Mercaptopropyl-functionalized silica mesostructures, denoted MP-HMS, were prepared through a S<sup>0</sup>I<sup>0</sup> supramolecular assembly pathway. Dodecyl-, tetradecyl-, hexadecyl-, and octadecylamine served as representative alkylamine surfactants (S<sup>0</sup>) for the assembly of 3-mercaptopropyltrimethoxysilane (MPTS) and tetraethyl orthosilicate (TEOS) as framework precursors (I<sup>0</sup>). The assembly process was investigated over the stoichiometric range 0.10–0.30: $x(1 - x)$  alkylamine:MPTS:TEOS, where  $x = 0.10 - 1.00$  represents the fraction of silicon centers that are MP-functionalized.

A survey of the reaction products formed at  $x = 0.30$ , S<sup>0</sup>/I<sup>0</sup> ratios in the range 0.10–0.30 and solvent compositions in the range from 100:0 to 20:80 (v/v) H<sub>2</sub>O:ethanol indicated that mercapto-functional HMS mesostructures with well-expressed wormhole framework structures and textural porosity were favored at S<sup>0</sup>/I<sup>0</sup> = 0.20–0.25 and a solvent composition of 90:10 (v/v) H<sub>2</sub>O:ethanol. Similar surfactant:reagent ratios and solvent compositions have been reported as being preferred for the assembly of purely inorganic HMS silicas.<sup>20–22</sup> Although HMS wormhole mesostructure formation was found to occur only for  $x \leq 0.60$  (see below), chemical analysis and <sup>29</sup>Si NMR indicated that essentially all of the organosilicon was incorporated into the reaction products whether they were mesostructured or not. For the product prepared at a reaction stoichiometry of  $x = 0.50$ , the yield was >95%. Also, the relative intensities of the <sup>29</sup>Si NMR resonances for the MP-SiO<sub>3</sub> and SiO<sub>4</sub> framework sites were equal within experimental uncertainty, and elemental analyses confirmed the NMR result. Thus, the assembly reaction was very nearly quantitative.

**Effect of Assembly Temperature and MPTS Loading.** To determine the effect of assembly temperature on the framework porosity and textural properties of MP-HMS silicas, assembly reactions were carried out at 25–65 °C. Dodecylamine was used as the surfactant, and the fraction of total silicon centers present as mercaptopropyl silane was maintained at  $x$  values of 0.10, 0.20, and 0.30. Each surfactant-free product exhibited a single low-angle XRD peak characteristic of a wormhole framework with a pore–pore correlation distance of 3.6–4.6 nm. The structural properties of these products are given in Table 1.

At low MP loadings ( $x = 0.10$ ), the framework pore sizes increased with increasing assembly temperature, although the surface area and total pore volume decreased. The benefits of a higher assembly temperature become more evident, however, at higher levels of MP functionalization where the framework pore size inevitably tended to decrease due to the presence of more MP groups in the framework. Even at an intermediate

(18) Macquarrie, D. J.; Jackson, D. B.; Tailaud, S.; Wilson, K.; Clark, J. H. *Stud. Surf. Sci. Catal.* **2000**, *129*, 275.

(19) Mercier, L.; Pinnavaia, T. J. *Chem. Mater.* **2000**, *12*, 188.

(20) Tanev, P. T.; Pinnavaia, T. J. *Science* **1995**, *267*, 865.

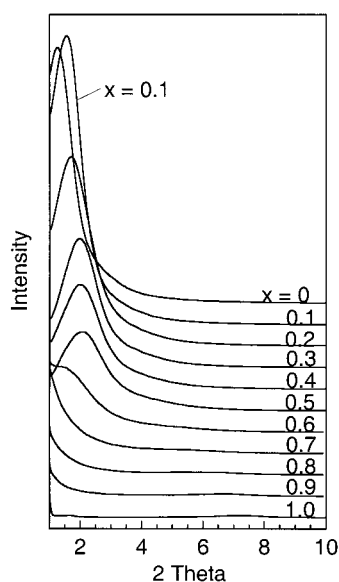
(21) Tanev, P. T.; Pinnavaia, T. J. *Chem. Mater.* **1996**, *8*, 2068.

(22) Zhang, W.; Pauly, T. R.; Pinnavaia, T. J. *Chem. Mater.* **1997**, *9*, 2491.

**Table 1. Effect of Assembly Temperatures on the Structural Properties of MP-HMS Mesostructures Assembled from  $x(1-x)$  MPTS:TEOS Mixtures<sup>a</sup>**

| $x$ | temp (°C) | $d_{001}$ (nm) | pore diam <sup>b</sup> (nm) | SA <sup>c</sup> (m <sup>2</sup> /g) | $V_t$ <sup>d</sup> (cm <sup>3</sup> /g) | $V_{fr}$ <sup>e</sup> (cm <sup>3</sup> /g) | $V_{tx}$ <sup>f</sup> (cm <sup>3</sup> /g) |
|-----|-----------|----------------|-----------------------------|-------------------------------------|---|--|--|
| 0.1 | 25        | 3.6            | 2.2                         | 1346                                | 1.39                                    | 0.62                                       | 0.77                                       |
| 0.1 | 45        | 4.6            | 2.7                         | 1162                                | 0.85                                    | 0.59                                       | 0.26                                       |
| 0.1 | 65        | 4              | 2.9                         | 880                                 | 0.67                                    | 0.54                                       | 0.13                                       |
| 0.2 | 25        | 3.4            | 1.8                         | 1198                                | 0.77                                    | 0.55                                       | 0.22                                       |
| 0.2 | 45        | 4.1            | 2.2                         | 1484                                | 1.27                                    | 0.68                                       | 0.59                                       |
| 0.2 | 65        | 4.1            | 2.3                         | 1095                                | 1.22                                    | 0.54                                       | 0.68                                       |
| 0.3 | 25        | 3.3            | <1.0                        | 928                                 | 0.52                                    | 0.44                                       | 0.08                                       |
| 0.3 | 45        | 3.7            | 2.1                         | 1286                                | 1.03                                    | 0.62                                       | 0.41                                       |
| 0.3 | 65        | 4.6            | 2                           | 1467                                | 1.94                                    | 0.73                                       | 1.21                                       |

<sup>a</sup> In each case dodecylamine was the structure director. <sup>b</sup> Determined by the Horvath–Kawazoe model. <sup>c</sup> Calculated by the Brunauer–Emmett–Teller (BET) method. <sup>d</sup> Total pore volume determined at  $P/P^0 = 0.98$ . <sup>e</sup> Framework pore volume determined at  $P/P^0 = 0.55$ . <sup>f</sup> Textural pore volume determined from the difference between  $V_t$  and  $V_{fr}$ .

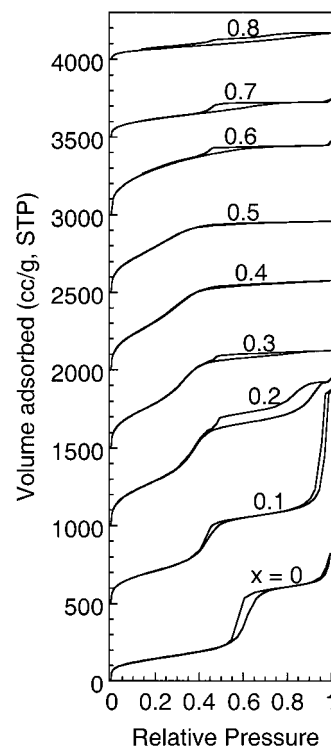
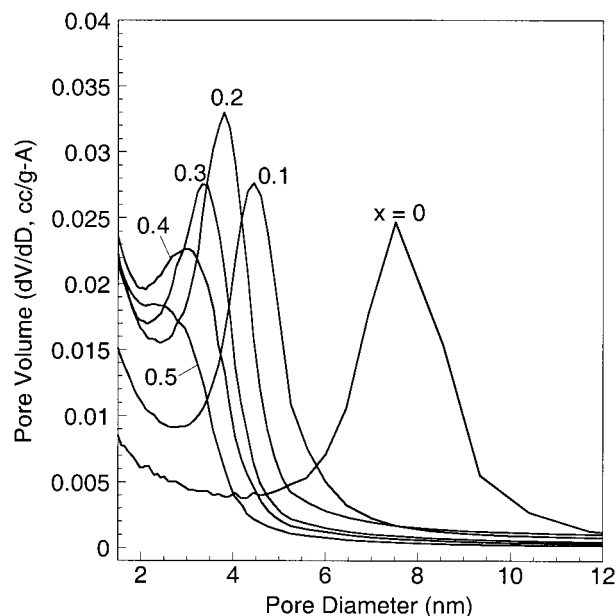
**Figure 1.** XRD patterns (Cu K $\alpha$ ) for the products formed at 65 °C from octadecylamine and  $x(1-x)$  MPTS:TEOS reaction mixtures.

MP loading of  $x = 0.30$ , the surface area, pore volume, and framework pore size all increased upon increasing the assembly temperature from 25 to 65 °C. Efforts to further enlarge the pore size of MP-HMS by increasing the assembly temperature beyond 65 °C, however, were unsuccessful. At assembly temperatures between 75 and 100 °C, mesostructure assembly at  $x = 0.30$  was compromised, as indicated by a dramatic loss of both the framework pore volume and the low-angle XRD peak. Therefore, the assembly of all subsequent MP-HMS mesostructures was carried out at 65 °C.

Regardless of the temperature for the assembly process, however, no wormhole mesostructure could be observed for products formed at MPTS:TEOS stoichiometries corresponding to  $x > 0.60$ . As shown by the powder diffraction patterns in Figure 1 for the products assembled at 65 °C using octadecylamine as the structure director, the pore to pore correlation peaks were absent for the compositions formed at  $x$  values above  $\sim 0.60$ , whereas below this value each product was clearly mesostructured.

#### Effect of Surfactant Chain Length on Porosity.

Figure 2 provides the N<sub>2</sub> isotherms for the mesostruc-

**Figure 2.** N<sub>2</sub> adsorption–desorption isotherms for mercaptopropyl-functionalized silicas formed at 65 °C from  $x$ MPTS and  $(1-x)$ TEOS mixtures in the presence of octadecylamine as the surfactant. Only the compositions with MP loadings  $x < 0.60$  are MP-HMS mesostructures.**Figure 3.** Horvath–Kawazoe pore size distributions obtained from the nitrogen adsorption isotherms of the MP-HMS mesostructures described in Figure 2.

ured MP-HMS compositions assembled from octadecylamine at  $x = 0.0$ – $0.60$ . Included for comparison are the isotherms for the nonstructured products obtained at  $x = 0.70$  and  $0.80$ . The Horvath–Kawazoe framework pore size distributions for the mesostructures, along with those assembled from shorter chain amines, are summarized in Table 2.



**Table 2. Dependence of MP-HMS Structural Properties on Surfactant Chain Length and MP Loading ( $x$ )<sup>a</sup>**

| amine surfactant | $x$  | $d_{001}$ (nm) | SA <sup>c</sup> (m <sup>2</sup> /g) | pore diam <sup>b</sup> (nm) | $V_t^d$ (cm <sup>3</sup> /g) | $V_{fr}^e$ (cm <sup>3</sup> /g) | $V_{tx}^f$ (cm <sup>3</sup> /g) |
|------------------|------|----------------|-------------------------------------|-----------------------------|------------------------------|---------------------------------|---------------------------------|
| dodecylamine     | 0.10 | 4.0            | 880                                 | 2.9                         | 0.67                         | 0.54                            | 0.13                            |
| tetradecylamine  | 0.10 | 5.3            | 800                                 | 3.6                         | 1.12                         | 0.73                            | 0.39                            |
| hexadecylamine   | 0.10 | 5.5            | 854                                 | 3.8                         | 1.45                         | 0.82                            | 0.63                            |
| octadecylamine   | 0.10 | 5.7            | 813                                 | 4.4                         | 2.14                         | 0.85                            | 1.29                            |
| dodecylamine     | 0.20 | 4.1            | 1095                                | 2.3                         | 1.22                         | 0.54                            | 0.67                            |
| tetradecylamine  | 0.20 | 4.9            | 1043                                | 2.8                         | 1.22                         | 0.64                            | 0.58                            |
| hexadecylamine   | 0.20 | 4.7            | 934                                 | 3.3                         | 1.20                         | 0.69                            | 0.51                            |
| octadecylamine   | 0.20 | 6.0            | 1157                                | 3.8                         | 1.47                         | 0.99                            | 0.48                            |
| dodecylamine     | 0.30 | 4.6            | 1467                                | 2.0                         | 1.94                         | 0.73                            | 1.21                            |
| tetradecylamine  | 0.30 | 4.3            | 1163                                | 2.6                         | 0.95                         | 0.60                            | 0.35                            |
| hexadecylamine   | 0.30 | 4.2            | 1202                                | 2.9                         | 0.79                         | 0.75                            | 0.04                            |
| octadecylamine   | 0.30 | 4.4            | 1191                                | 3.3                         | 0.97                         | 0.87                            | 0.10                            |
| dodecylamine     | 0.40 | 4.4            | 1077                                | 1.9                         | 1.02                         | 0.51                            | 0.51                            |
| tetradecylamine  | 0.40 | 4.3            | 1198                                | 2.4                         | 0.68                         | 0.59                            | 0.09                            |
| hexadecylamine   | 0.40 | 4.3            | 1257                                | 2.7                         | 0.76                         | 0.70                            | 0.06                            |
| octadecylamine   | 0.40 | 4.3            | 1319                                | 3.0                         | 0.89                         | 0.84                            | 0.05                            |
| dodecylamine     | 0.50 | 4.9            | 695                                 | ---                         | 0.34                         | 0.32                            | 0.03                            |
| tetradecylamine  | 0.50 | 4.8            | 913                                 | 2.2                         | 0.50                         | 0.45                            | 0.05                            |
| hexadecylamine   | 0.50 | 4.6            | 855                                 | 2.4                         | 0.54                         | 0.44                            | 0.10                            |
| octadecylamine   | 0.50 | 4.3            | 1225                                | 2.8                         | 0.71                         | 0.69                            | 0.02                            |

<sup>a</sup> Each mesostructure was assembled from  $x(1-x)$  MPTS:TEOS mixtures in 90:10 (v/v) H<sub>2</sub>O/ethanol at 65 °C. <sup>b</sup>—<sup>f</sup>These footnotes are the same as those given in Table 1.

Although the framework pore size of a MP-HMS silica decreases with increasing MP loading, the pore size obtained at a specific MP loading increases with increasing chain length of the surfactant, as expected. As can be seen from the results presented in Table 2, octadecylamine affords pore diameters that are 1.0–1.5 nm larger than those obtained from dodecylamine at MP loadings of  $x = 0.10$ – $0.40$ . Even at  $x = 0.5$ , octadecylamine affords a mesoporous MP-HMS with a pore diameter of 2.8 nm.

It is noteworthy that the textural porosity ( $V_{tx}$ ) of MP-HMS silicas, which arises from the spongelike nature of the particles,<sup>22</sup> decreases rapidly with increasing MP loading. Substituting just 10% of the framework silicon centers with mercaptopropylsilyl groups reduces the pore sizes from 7.5 nm ( $x = 0$ ) to 4.4 nm ( $x = 0.10$ ), while the textural porosity is increased dramatically from 0.33 to 1.29 cm<sup>3</sup>/g. As the MP functionalization is increased, however, the size of the spongelike textural pores decreases, as indicated by the broadening of the hysteresis loop. At  $x$  values above 0.30, the spongelike textural porosity is lost.

The variation in the textural porosity with retention of a wormhole framework structure over the range  $x = 0$ – $0.40$  was verified by the high- and low-magnification images shown in Figure 4. Intergrown mesoscopic wormhole domains and spongelike particle textures are clearly evident in the low-magnification micrographs for  $x = 0$ , 0.10, and 0.20. As the value of  $x$  increases, the domains become smaller and more completely intergrown. At  $x = 0.30$ – $0.40$  the domains are completely intergrown, the particle texture becomes monolithic, and the spongelike textural mesoporosity is lost (cf., Figures 2 and 4).

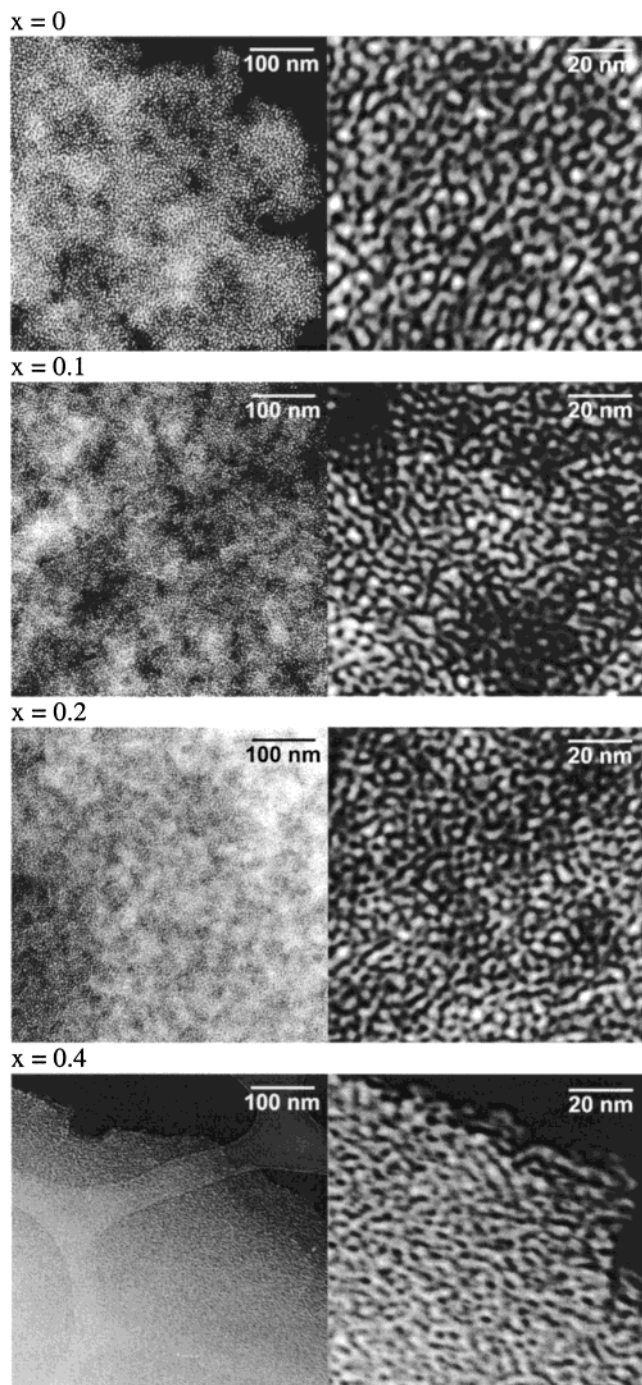
**Framework Cross-linking.** Figure 5 provides a typical <sup>29</sup>Si MAS NMR spectrum for a MP-HMS silica assembled from dodecylamine as the surfactant and at an  $x$  value of 0.30. The resonances near  $-100$  and  $-111$  ppm represent the Q<sup>3</sup> OSi(OSi)<sub>3</sub> and Q<sup>4</sup> Si(OSi)<sub>4</sub> environments of the SiO<sub>4</sub>, whereas the  $-59$  and  $-68$  ppm signals arise from the T<sup>2</sup> and T<sup>3</sup> connectivities of the MP-functionalized silicon centers.

Table 3 reports the framework cross-linking parameters Q<sup>4</sup>/Q<sup>3</sup> and (Q<sup>4</sup> + T<sup>3</sup>)/(Q<sup>3</sup> + T<sup>2</sup>) for representative MP-HMS mesostructures. Note that the framework cross-linking increases with the assembly temperature as well as with the degree of MP functionalization. Approximately half of the silicon sites are fully cross-linked in a 10% -functionalized MP-HMS mesostructure assembled at 25 °C. In contrast, ~90% of the framework silicon centers are fully cross-linked in a MP-HMS assembled at 65 °C and MP loadings of 40–50%. The degree of framework cross-linking could be increased an additional ~5–10% by a postsynthesis treatment of the as-made mesostructures at 100 °C for 24–72 h.

## Discussion

Previous efforts to prepare MP-functionalized mesostructures by direct assembly methods have been limited to compositions in which fewer than 30% of the framework silicon centers are actually functionalized. Stein<sup>9</sup> achieved 28.5% MP functionalization for the direct assembly of MP-MCM-41, but in this case the hexagonal structure was *microporous*. Mesoporous MP-MCM-41 derivatives, however, were limited to 20–30% framework functionalization, depending on the relative hydrolysis rates of the organosilane and siloxane precursors.<sup>9,16</sup> Limited levels of MP functionalization (10–20%) also have been reported for hexagonal SBA-15 mesostructures that assemble under acidic assembly conditions using a nonionic surfactant as the structure director.<sup>15</sup> Similar low levels of MP functionalization have been reported for silicas with wormhole framework structures, whether of the HMS type formed from alkylamines<sup>7,19,11,18</sup> or of the MSU-X variety assembled from nonionic surfactants.<sup>8,23</sup> Although organo-silica compositions have been reported in which up to 50% of the silicon sites has been MP-functionalized, these materials lack framework mesoporosity, as judged by both XRD and nitrogen adsorption.<sup>18</sup>

The S<sup>0</sup>I<sup>0</sup> assembly processes described in the present work afforded well-expressed wormhole mesostructures



**Figure 4.** Transmission electron micrographs of representative MP-HMS mesostructures assembled at 65 °C from octadecylamine, showing at low magnification the spongelike particle texture obtained at MP loadings of  $x = 0$ –0.20 and the monolithic texture obtained for  $x = 0.40$ . The high-magnification images verify the wormhole framework structure.

in which at least 50% of the framework silicon sites could be MP-functionalized with retention of the pore size, pore volume, and surface area with values as high as 2.8 nm, 0.69 cm<sup>3</sup>/g, and 1225 m<sup>2</sup>/g, respectively. Depending on the choice of amine surfactant MP-HMS at 60% functionalization may or may not exhibit well-expressed XRD peaks and framework pore size distributions. Nevertheless, 60% MP-HMS assembled from octadecylamine exhibited the same pore volume and surface area values (2.6 nm, 0.68 cm<sup>3</sup>/g, and 1133 m<sup>2</sup>/g,

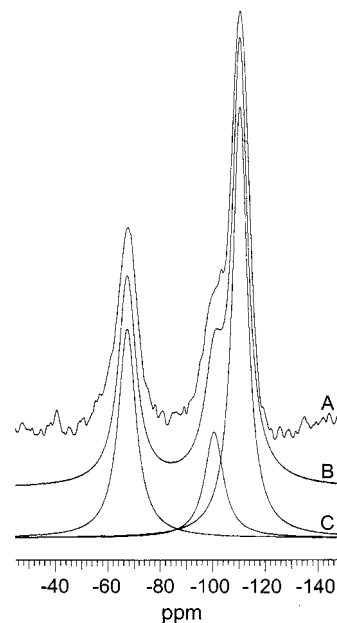


**Figure 5.** Representative <sup>29</sup>Si MAS NMR spectra for a MP-HMS mesostructure assembled at 65 °C from octadecylamine and a MP loading of  $x = 0.30$ : (A) observed spectrum; (B) simulated spectrum; (C) deconvoluted resonance components of the simulated spectrum.

**Table 3.** <sup>29</sup>Si MAS NMR Cross-linking Parameters for MP-HMS Silicas Assembled from Alkylamine Surfactants and  $x(1 - x)$  MPTS:TEOS Mixtures

| amine surfactant                                | $x$  | assembly temp (°C) | Q <sup>4</sup> /Q <sup>3</sup> | (Q <sup>4</sup> + T <sup>3</sup> )/(Q <sup>3</sup> + T <sup>2</sup> ) |
|---|------|--------------------|--------------------------------|---|
| C <sub>12</sub> H <sub>25</sub> NH <sub>2</sub> | 0.10 | 25                 | 1.20                           | 1.15  |
|   | 0.30 | 65                 | 3.24                           | 5.13  |
| C <sub>16</sub> H <sub>29</sub> NH <sub>2</sub> | 0.10 | 45                 | 1.41                           | 1.56  |
|   | 0.40 | 45                 | 2.26                           | 4.16  |
| C <sub>18</sub> H <sub>37</sub> NH <sub>2</sub> | 0.10 | 65                 | 2.42                           | 2.66  |
|   | 0.30 | 65                 | 3.77                           | 5.59  |
|   | 0.40 | 65                 | 4.92                           | 8.25  |
|   | 0.50 | 65                 | 5.56                           | 10.32   |

respectively) as the 50% material, although the pore distribution extended into the microporous range (~1.0–2.5 nm). Thus, although the degree of wormhole framework ordered decreases above ~60% MP functionalization and results in the broadening and eventual loss of a pore–pore correlation peak in the XRD, some accessible porosity and surface area is retained, even for these highly disorder compositions.

The key to the preparation of these highly functionalized derivatives lies in the use of long-chain alkylamine surfactants as structure directors (e.g., octadecylamine) in combination with a relatively high assembly temperature (e.g., 65 °C). Also, it is important to use a solvent of high polarity, for example, 90:10 (v/v) H<sub>2</sub>O: ethanol. Low-polarity solvents, for example, 63:37 (v/v) H<sub>2</sub>O: ethanol, were only marginally useful in forming mesostructures at low MP loading ( $x = 0.10$ ) and completely ineffective in generating an organo-functional mesostructure at  $x$  values above ~0.20. Apparently, a high-polarity solvent favors the partitioning of the organosilane precursor at the surfactant–micelle interface. Similar partitioning effects may also explain the observation that mesitylene, which often is used as a pore-expanding agent in mesostructure assembly, is ineffective in swelling MP-HMS mesopores at low MP

loading ( $x \sim 0.10$ ) and even inhibits mesostructure assembly at high loading ( $x \sim 0.30$ ).

Earlier studies of MP-HMS synthesis utilized relatively short chain alkylamines (e.g., dodecylamine) and lower assembly temperatures. The larger amines used in the present work expand the pore size to allow for the accommodation of more MP groups on the framework walls. The higher assembly temperature provides a better balance of the hydrolysis and condensation reactions of the siloxane precursors for mesostructure formation as well as the enhancement of the framework pore size. The increase in framework pore size with increasing assembly temperature is attributable to a reduced level of hydration at the amine-silica interface, which lowers the surfactant packing parameter and, consequently, the curvature of the micelle. Too high an assembly temperature, however, is detrimental to mesostructure formation through  $S^0I^0$  assembly pathways.  $S^0I^0$  assembly relies on H bond formation between the amine surfactant ( $S^0$ ) and siloxane precursors ( $I^0$ ) at the micelle interface. If the thermal energy is too large, the H bonding is compromised, and little or no mesostructure is formed.

Another advantage of a higher  $S^0I^0$  assembly temperature is the improvement realized in the degree of framework cross-linking. As indicated by the cross-linking parameters in Table 3, 70% of the silicon centers for the MP-HMS assembled at 65 °C are fully cross-linked at  $x = 0.10$ . The number of completely cross-linked centers increases to ~90% at  $x = 0.40$ – $0.50$ . To our knowledge this is the highest level of framework cross-linking achieved for an organo-functional silica mesostructure. The relationship between framework cross-linking and the extent of framework functionalization is attributable to a decrease in the hydration of the  $S^0$ – $I^0$  micelle interface as the number of organo groups increases at this interface. The enhanced framework cross-linking leads to substantial improvements in hydrothermal stability, which can be important for applications involving metal ion trapping in hot water. For instance, MP-HMS mesostructures at MP loadings of 40–50% are stable with boiling water for at least 10 h, whereas purely inorganic HMS silicas degrade substantially under these conditions. Future studies will report on the trapping of  $Hg^{2+}$  by highly functionalized MP-HMS mesostructures.

The improved hydrothermal stability for MP-HMS should also be important in converting the immobilized mercapto groups to sulfonic acid moieties. Previously reported studies indicate that substantial framework degradation occurs upon the nitric acid<sup>9</sup> oxidation of MP-MCM-41. In contrast, our preliminary studies indicate that the peroxide oxidation of mercapto groups in MP-HMS at 50% functionalization ( $x = 0.50$ ) can be achieved with complete retention of the mesostructure. The retention of mesoporosity, together with a high sulfonic acid loading, should prove to be advantages in liquid catalytic applications, such as monoglyceride synthesis, where facile access to active sites is important in determining product selectivity.<sup>12</sup>

The  $S^0I^0$  assembly processes described here have provided unprecedented mercaptopropyl loading of up to ~5.6 mmol/g, equivalent to multi-molar homogeneous solutions. It is likely that analogous assembly methods will provide HMS mesostructures containing exceptionally high levels of other organo-functional groups for improved catalytic applications. Organo-substituted HMS wormhole structures have been shown to be especially active catalysts in comparison to two-dimensional hexagonal mesostructures for a variety of "green" organic transformations, including the Baeyer-Villiger oxidation of ketones,<sup>24</sup> Michael additions,<sup>25</sup> among several others.<sup>26,27</sup> Even greater catalytic reactivity can be anticipated for these wormhole structures by increasing the organo-functional group loading to the levels achieved in the present work.

**Acknowledgment.** Y.M. wishes to thank Mitsubishi Chemical Co. for financial assistance in support of an educational leave of absence. The partial support of this research through NIEHS Grant ESO4911C is gratefully acknowledged. Also, equipment purchased under NSF-CRG Grant 9903706 was used in support of this work.

CM010048R

(24) Lambert, A.; Elings, J. A.; Macquarrie, D. J.; Carr, G.; Clark, J. H. *Synlett* **2000**, 1052.

(25) Mdoe, J. E. G.; Clark, J. H.; Macquarrie, D. J. *Synlett* **1998**, 625.

(26) Macquarrie, D. J. *Green Chem.* **1999**, *1*, 195.

(27) Clark, J. H.; Macquarrie, D. J. *Chem. Commun.* **1998**, 853.